

## Resonant inelastic x-ray scattering on single magnons at oxygen $K$ edges

Beom Hyun Kim and Jeroen van den Brink

*Institute for Theoretical Solid State Physics, IFW Dresden, Helmholtzstrasse 20, 01069 Dresden, Germany*

(Received 7 April 2014; revised manuscript received 7 July 2015; published 10 August 2015)

The recent discovery that resonant inelastic x-ray scattering can probe single-magnon (SM) dispersions in transition metal (TM) oxides when the x-ray energy is tuned to the TM  $L$  edge has put this technique on a par with inelastic neutron scattering. It is generally presumed that selection rules forbid SM scattering at oxygen (O)  $K$  edges. However, based on a symmetry analysis and exact diagonalization study, we show that SM scattering at O  $K$  edges becomes allowed when (i) spin-orbit coupling is present in the TM  $d$  shell and (ii) inversion symmetry at the O site is broken. For cuprates the resulting SM amplitude is very weak, but in iridates both prerequisites can amply be fulfilled.

DOI: [10.1103/PhysRevB.92.081105](https://doi.org/10.1103/PhysRevB.92.081105)

PACS number(s): 75.30.Ds, 71.70.Ej, 78.70.Ck

**Introduction.** The theoretical prediction [1] and subsequent experimental observation [2,3] that the dispersion of magnetic excitations, in particular, of elementary single magnons, can be measured directly by resonant inelastic x-ray scattering (RIXS) has fundamentally changed the field of inelastic magnetic scattering [4]. It has, for instance, led to the discovery of distinct paramagnons in a large family of high-temperature cuprate superconductors [3–8], and established the presence of strongly dispersive magnetic modes in a number of iridium oxides [9–12].

All these efforts to extract the dispersion of elementary magnetic excitations from RIXS have focused on the transition metal (TM)  $L$  edge, where single spin-flip scattering is directly allowed [1–16]. The microscopic origin of this type of magnetic scattering is rather straightforward. When the incoming photon energy is tuned to a TM  $L$ -edge energy in RIXS, an electron with spin  $\sigma$  is excited out of the atomic  $p$  shell, deep inside the atomic core, into the TM  $d$  shell. The core hole that is created in this event can now flip its spin due to its very large spin-orbit interaction. Subsequently, a valence  $d$  electron with spin  $-\sigma$  can fill the core hole and an outgoing x ray is emitted. The net result of this RIXS process is a spin-flip transition  $\sigma \rightarrow -\sigma$  in the TM  $d$  shell, which is the same as the net result of inelastic neutron scattering involving this  $d$ -shell electron.

When a  $K$  edge is used instead of an  $L$  edge, this direct spin-flip process is no longer allowed. This is because in  $K$ -edge RIXS an electron is excited from a core shell with  $s$  symmetry, for which spin-orbit coupling is simply absent. It thus appears that for RIXS at  $K$  edges, direct spin-flip scattering is forbidden and only higher-order magnetic scattering processes—starting at double spin-flip (e.g., bimagnon) scattering—are allowed [17–19]. Indeed, bimagnon scattering is observed both at TM [20,21] and oxygen (O)  $K$  edges [22,23]. This apparent absence of single-magnon spin-flip scattering is unfortunate because the O  $K$  edge is in a soft x-ray regime where the RIXS resolution is particularly high (even if in this situation only a limited part of momentum space is accessible) and oxygen anions are obviously ubiquitous in magnetic materials.

However, in this Rapid Communication we show that single-magnon (SM) scattering at O  $K$  edges is allowed when spin-orbit coupling is present in the TM  $d$  shell and inversion symmetry at the O site is broken. Our symmetry analysis and exact diagonalization study show that the resulting SM

scattering is allowed for small momentum losses and forbidden for momenta close to the magnetic ordering vector, a situation opposite to magnetic RIXS at the TM  $L$  edge. As the spin-orbit interaction in the  $5d$  shell is large and the inversion symmetry at O sites is often distinctly broken in iridates, as, e.g., in the perovskites  $\text{Sr}_2\text{IrO}_4$ ,  $\text{Sr}_3\text{Ir}_2\text{O}_7$ , and  $\text{Na}_2\text{IrO}_3$ , and the postperovskite  $\text{CaIrO}_3$ , we predict pronounced SM scattering at the O  $K$  edge of, for instance, these magnetic oxides.

**RIXS cross section.** When an incident (outgoing) x ray with  $\epsilon$  ( $\epsilon'$ ) polarization has the frequency  $\omega_{\mathbf{k}}$  ( $\omega_{\mathbf{k}'}$ ) and wave vector  $\mathbf{k}$  ( $\mathbf{k}'$ ), the RIXS intensity is described by the Kramers-Heisenberg relation [4]

$$I(\omega, \mathbf{q}, \epsilon, \epsilon') = \sum_f |\mathcal{F}_{fg}(\omega, \mathbf{q}, \epsilon, \epsilon')|^2 \times \delta(E_f + \hbar\omega_{\mathbf{k}} - E_g - \hbar\omega_{\mathbf{k}'}), \quad (1)$$

where  $\omega = \omega_{\mathbf{k}} - \omega_{\mathbf{k}'}$  and  $\mathbf{q} = \mathbf{k} - \mathbf{k}'$ . In the dipole and fast collision approximation, the scattering amplitude  $\mathcal{F}_{fg}$  is reduced to  $\mathcal{F}_{fg} = \frac{1}{i\Gamma} \langle f | R(\epsilon', \epsilon, \mathbf{q}) | g \rangle$ , where  $R$  is the effective RIXS scattering operator, which is defined by the product of two dipole operators, and  $\Gamma$  is the core-hole broadening [4]. When  $\psi_v$  and  $\psi_s$  represent valence and core states, the scattering operator is given by

$$R(\epsilon', \epsilon, \mathbf{q}) = \sum_{i\nu\nu'} e^{i\mathbf{q}\cdot\mathbf{r}_i} T_{\nu'\nu}(\epsilon', \epsilon) c_{i\nu'} c_{i\nu}^\dagger, \quad (2)$$

where  $T_{\nu'\nu}(\epsilon', \epsilon) = \sum_s \langle \psi_{\nu'} | \epsilon' \cdot \mathbf{r} | \psi_s \rangle \langle \psi_s | \epsilon \cdot \mathbf{r} | \psi_\nu \rangle$ . In case of the O  $K$ -edge RIXS,  $T_{\nu'\nu}(\epsilon', \epsilon)$  equals  $\frac{1}{3} \epsilon_{m'} \epsilon_m \delta_{\sigma', \sigma} \langle r \rangle^2$ , where  $\nu$  has  $m$  ( $x$ ,  $y$ , or  $z$ ) orbital and  $\sigma$  spin characters. The most important feature of the O  $K$ -edge RIXS process is that in its intermediate state, besides an oxygen core hole, an extra valence electron is also present that hybridizes and interacts with the TM  $d$  electrons.

**Symmetry analysis.** To investigate the magnetic response of the O  $K$ -edge RIXS, we start by considering a simple periodic TM1-O1-TM2-O2 arrangement of transition metal and oxygen ions, where the TM-O-TM bond angle is  $\phi$  (see Fig. 1). To be specific, we concentrate on iridates (cuprates) in the following symmetry analysis, in which the  $\text{Ir}^{4+}$  ( $\text{Cu}^{2+}$ ) ions are in a  $5d^5$  ( $3d^9$ ) configuration. Due to the strong spin-orbit coupling,  $\text{Ir}^{4+}$  ions in iridates form effective  $J_{\text{eff}} = 1/2$  moments [24,25] so that the single-site ground-state multiplet is a Kramers doublet, which we denote by  $D$ . Also in the case of  $\text{Cu}^{2+}$  in

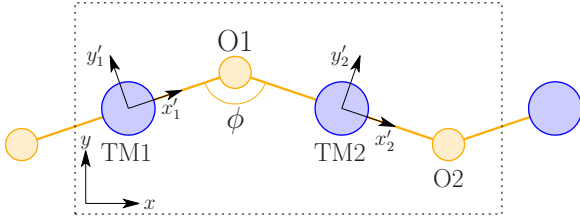


FIG. 1. (Color online) Schematic diagram of a corner-sharing TM-O system, which for bond angle  $\phi$  not equal to  $180^\circ$  lacks inversion symmetry at the oxygen site. The  $z$  direction is out of plane.

cuprates, a Kramers doublet ( $S = 1/2$ ) is the ground state as the tetragonal crystal field splits up the  $e_g$  orbital degeneracy. When one considers two of these moments, the magnetic interactions between them cause a splitting into a total singlet ( $S$ ) and a total triplet ( $T$ ) state. The four states are  $|S\rangle = \frac{1}{\sqrt{2}}(|D_\uparrow D_\downarrow; 00\rangle - |D_\downarrow D_\uparrow; 00\rangle)$ ,  $|T_1\rangle = |D_\uparrow D_\uparrow; 00\rangle$ ,  $|T_0\rangle = \frac{1}{\sqrt{2}}(|D_\uparrow D_\downarrow; 00\rangle + |D_\downarrow D_\uparrow; 00\rangle)$ , and  $|T_{-1}\rangle = |D_\downarrow D_\downarrow; 00\rangle$ , where  $|00\rangle$  denotes the *absence of holes* on the oxygen sites, in the  $O$   $p$  orbitals. Because of the hopping  $t_{pd}$  between TM and O, such charge-transfer states of course mix in. We denote such a charge-transfer state with a hole on oxygen as  $|D_\sigma A; \xi 0\rangle$ , where  $A$  represents the Ir  $5d^6$  (Cu  $3d^{10}$ ) state, in which all doublet states are occupied, and  $\xi$  refers to the  $p$ -hole state of O.

We now introduce two different inversion symmetry operators  $I_O$  and  $I_{TM}$  that represent inversion with respect to O and TM centers, respectively. When  $I_O$  and  $I_{TM}$  are applied, local coordinates transform as  $I_O : (x'_1, y'_1) \rightarrow (-x'_2, -y'_2), (x_1, y_1) \rightarrow (-x_1, -y_1)$  and  $I_{TM} : (x'_1, y'_1) \rightarrow (-x'_1, -y'_1), (x_1, y_1) \rightarrow (-x_2, -y_2)$ . We note that  $I_{TM}$  is *always* a symmetry of the system, but  $I_O$  is a symmetry operator *only for*  $\phi = 180^\circ$ , i.e., undistorted TM-O-TM bonds. Because of  $I_{TM}$  symmetry, the hopping integrals between singlet or triplet and charge-transfer states obey the relations  $\langle S|H_t|D_\sigma A; \xi 0\rangle = -\langle S|H_t|D_\sigma A; 0\xi\rangle$  and  $\langle T_m|H_t|D_\sigma A; \xi 0\rangle = -\langle T_m|H_t|D_\sigma A; 0\xi\rangle$ , where  $H_t$  is the TM-O hopping part of the Hamiltonian, so that the singlet ground state  $|g\rangle$  and triplet excited states  $|m\rangle$  become

$$|g\rangle = c|S\rangle + \sum_{\sigma\xi} c_{\sigma\xi}(|D_\sigma A; \xi 0\rangle - |D_\sigma A; 0\xi\rangle) + \dots,$$

$$|m\rangle = c_m|T_m\rangle + \sum_{\sigma\xi} c_{m\sigma\xi}(|D_\sigma A; \xi 0\rangle - |D_\sigma A; 0\xi\rangle) + \dots,$$

which directly follows from the symmetry properties of the states involved, given explicitly in Table I.

Next, we require the symmetry properties of the effective RIXS scattering operator  $R(\epsilon', \epsilon, \mathbf{q})$  in Eq. (2) under inversion. These explicitly depend on the momentum  $\mathbf{q}$  that is transferred by an x-ray photon to the system: Only for momenta corresponding to high symmetry points in the Brillouin zone (BZ) is a symmetry analysis viable, in the present case, in particular, for  $q = 0$  and  $q = \pi$ . For these momenta, the transformation properties of  $R$  under the two types of inversion,  $I_O$  and  $I_{TM}$ , are summarized in Table II, considering both RIXS at the O  $K$  edge and the Ir  $L_3$  edge.

TABLE I. Transformation properties of singlet ( $|S\rangle$ ), triplet ( $|T\rangle$ ), and charge-transfer ( $|D_\sigma A; \xi 0\rangle$ ) states under two types of inversion,  $I_O$  and  $I_{TM}$ . Note that  $I_O$  is only a symmetry when the bond angle  $\phi = 180^\circ$ .

	$ S\rangle$	$ T\rangle$	$ D_\sigma A; \xi 0\rangle$
$I_O (\phi = 180^\circ)$	$- S\rangle$	$ T\rangle$	$- AD_\sigma; \xi 0\rangle$
$I_M$	$ S\rangle$	$ T\rangle$	$- DA_\sigma; 0\xi\rangle$

Having determined these transformation properties, it can be immediately verified that the RIXS scattering amplitude  $\mathcal{F}_{mg}^{OK}$  at the O  $K$ -edge between the ground state  $|g\rangle$  and magnetically excited state  $|m\rangle$  obeys the selection rule  $\mathcal{F}_{mg}^{OK}(q = \pi) = 0$  for all  $m$ , because  $I_{TM}^\dagger R(q = \pi) I_{TM} = -R$ . For  $q = 0$  no such selection rule is dictated by  $I_{TM}$ . However, in the situation where the bond angle is  $180^\circ$  and  $I_O$  is a symmetry of the system, the relations  $\langle S|H_t|D_\sigma A; \xi 0\rangle = \langle S|H_t|AD_\sigma; \xi 0\rangle$  and  $\langle T_m|H_t|D_\sigma A; \xi 0\rangle = -\langle T_m|H_t|AD_\sigma A; \xi 0\rangle$  hold, which imply that, in addition,  $\mathcal{F}_{mg}^{OK}(q = 0) = 0$ . Conversely, this implies that magnetic scattering at the O  $K$  edge is *allowed* at  $q = 0$  and its vicinity when  $\phi \neq 180^\circ$  and inversion symmetry at the O site is broken.

It is interesting to perform an analog symmetry analysis for magnetic RIXS at the  $L$ -edge RIXS. The scattering amplitude  $\mathcal{F}_{mg}^L$  is proportional to  $c^* c_m \langle T_m | R | S \rangle$  and it can easily be verified that  $I_{TM}$  does not give rise to any selection because both  $|S\rangle$  and  $|T_m\rangle$  have the same parity under  $I_{TM}$ . Interestingly, for straight bonds with  $\phi = 180^\circ$ , where  $I_O$  is a symmetry of the system,  $\mathcal{F}_{mg}^L(q = 0) = 0$ . This is related to the fact that for  $I_O$  the singlet and triplet states have different parities. These selection rules are of course directly related to the experimental and theoretical observations that on iridates and cuprates the magnetic  $L$ -edge RIXS intensity peaks at the edge of the BZ [2,3,10–12].

*Exact diagonalization results.* In order to test these symmetry-based selection rules and to determine in addition their dependence on the incoming and outgoing polarization of x-ray photons, we perform an exact diagonalization (ED) study of the relevant microscopic model Hamiltonian for iridates and cuprates on small clusters. The generic Hamiltonian is  $H = \sum_{ij} H_i^{\text{TM}} + H_j^{\text{O}} + H_{ij}^t$ , where  $H_i^{\text{TM}}$  and  $H_j^{\text{O}}$  refer to the local Hamiltonian of TM and O ions on neighboring sites  $i$  and  $j$  and  $H_{ij}^t$  captures the hopping of electrons on the connecting TM-O bond [26]. Further details are provided in the Supplemental Material [27–29]. We calculate the RIXS intensity with the help of the Kubo formula of the scattering operator given by Eq. (2).

TABLE II. Symmetry properties of RIXS scattering operator  $R$  at the O  $K$  edge and Ir  $L_3$  edge with respect to two types of inversions,  $I_O$  and  $I_{TM}$ .

	Ir $L$ edge		O $K$ edge	
	$q = 0$	$q = \pi$	$q = 0$	$q = \pi$
$I_O (\phi = 180^\circ)$	$R$	$-R$	$R$	$R$
$I_{TM}$	$R$	$R$	$R$	$-R$

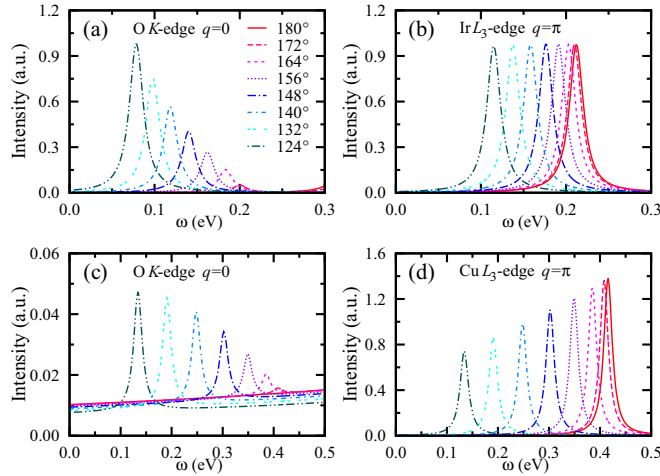


FIG. 2. (Color online) Magnetic RIXS spectra calculated by ED as a function of TM-O-TM bond angle  $\phi$ . (a) Ir iridate O  $K$  edge at  $q = 0$ , (b) Ir  $L_3$  edge at  $q = \pi$ , (c) cuprate O  $K$  edge RIXS at  $q = 0$ , and (d) Cu  $L_3$  edge at  $q = \pi$ . The polarizations are  $\epsilon = x$  and  $\epsilon' = z$ . Note that, as a function of  $\phi$ , both the effective magnetic interactions and the RIXS intensity change.

The RIXS spectra, calculated as a function of the TM-O bond angle  $\phi$ , are shown in Fig. 2, where the two top panels are the results for an  $\text{Ir}^{4+}$  cluster and the two lower panels are for a  $\text{Cu}^{2+}$  cluster, with, on the left, the magnetic scattering at the oxygen  $K$  edges and, on the right, RIXS intensities at the TM  $L$  edges [30]. There are many charge excitations at higher energy, but we focus on only the low-energy magnetic part of the excitation spectra. The overall trends are very similar. First of all, it is clear that when  $\phi$  starts to deviate from  $180^\circ$ , the energy of the magnetic excitations goes down, which is due to the reduction of the effective exchange interaction between the (iso)spins, as the hopping integrals directly depend on the bond angle. This is equally true for RIXS at the Ir or Cu  $L$  edges and at the corresponding O  $K$  edges. A big difference is, however, that for straight bonds, where  $\phi = 180^\circ$ , the O  $K$ -edge magnetic scattering intensity vanishes, whereas the TM  $L$ -edge intensity is finite in both cases. This is the result of the selection rules derived above. Only when the bond angle  $\phi$  begins to deviate from  $180^\circ$  does the magnetic RIXS intensity start to build up at the O  $K$  edge. It should be noted, however, that for typical parametrizations of quasi-two-dimensional (2D) perovskite iridates and cuprates, the magnetic scattering intensity at the oxygen edge is at least  $\sim 20$  times larger in the iridate compared to the cuprate. This reflects the fact that the spin-orbit coupling in iridates is much larger.

It is interesting to analyze the polarization dependence of the RIXS amplitude for an iridate with buckled bonds. The polarization directions of the incoming ( $\epsilon$ ) and outgoing ( $\epsilon'$ ) x rays are defined in the coordinate system of Fig. 1 and the resulting RIXS spectra shown in Fig. 3. It should first of all be noted that there are two sets of magnetic excitations because of the additional anisotropic interactions (Dzyaloshinskii-Moriya and Kitaev exchange terms) that are generated by the buckling of bonds [27,31], splitting up the excited magnetic states. At the Ir  $L$  edge, one set of magnetic modes is picked up in  $yz$  and  $zy$  polarization, and the other four orthogonal polarization

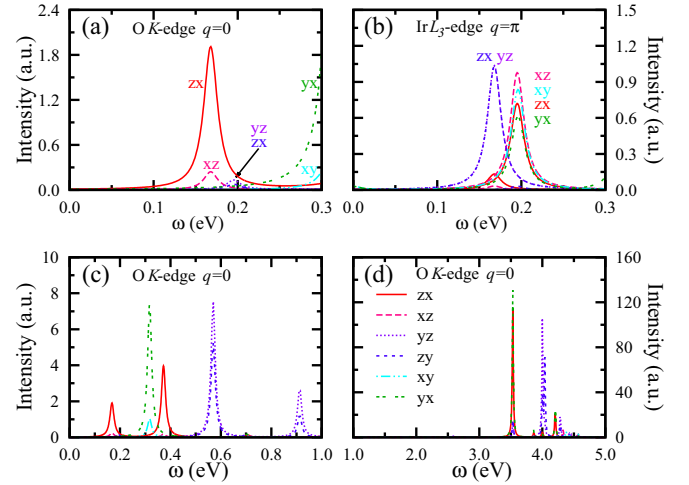


FIG. 3. (Color online) Polarization dependence of magnetic RIXS excitations for an iridate cluster with an Ir-O-Ir bond angle of  $\phi = 158^\circ$ . (a) O  $K$  edge at  $q = 0$  and (b) Ir  $L_3$  edge at  $q = \pi$ . The polarization condition  $zx$  labels  $\epsilon = z$ ,  $\epsilon' = x$ . The O  $K$ -edge RIXS spectra at  $q = 0$  below 5.0 eV are presented in (c) and (d). RIXS peaks from 0.3 to 1.0 eV and above 3.0 eV are attributed to local  $dd$  excitations and charge-transfer excitations, respectively.

conditions pick up the other magnetic mode. The magnetic scattering is only present in cross-polarization conditions, which reflects the fact that in SM scattering the angular momentum is transferred from the x-ray photon to the magnon. This is also reflected in the O  $K$ -edge RIXS, where, depending on the specific polarization conditions, either of the magnetic modes is picked up ( $zx, xz$  vs  $yz, zy$ ), or none ( $yx$  and  $xy$ ). Note that the magnetic scattering intensity is by far largest for the situation of incoming polarization in the  $z$  direction and outgoing polarization along the  $x$  axis. Note that in the spectra we do not show the elastic contribution to the resonant scattering, which in principle produces a zero-loss peak.

At energies above the magnetic excitations, local  $dd$  transitions, referred to as spin-orbit excitons in iridates [10], and charge-transfer excitations are present. As shown in Figs. 3(c) and 3(d), the RIXS spectra show peaks from 0.3 to 1.0 eV ( $dd$  transitions) and above 3.0 eV (charge-transfer excitations). It is clear that the charge-transfer peaks provide the most RIXS intensity, about two orders of magnitude stronger than the magnetic excitations, which in turn have intensities that are weaker than, but of the same order of magnitude as, the spin-orbit excitons.

It is clear that the calculated magnetic RIXS intensity at the oxygen  $K$  edge of iridates, apart from symmetry, critically depends on an interplay of the spin-orbit coupling and the hybridization between oxygen  $p$  and iridium  $d$  states—without either one or the other, the magnetic RIXS intensity vanishes. In the cluster the Ir-O hopping is parametrized by  $t_{pd\sigma}$ , and the magnetic scattering intensity as a function of  $t_{pd\sigma}$  is shown in Fig. 4 on a log-log scale for a fixed bond angle of  $158^\circ$ . It makes clear that there are two types of contributions to the intensity, scaling with  $t_{pd\sigma}^4$  and  $t_{pd\sigma}^8$ , respectively, in the weak hopping limit. Moreover, which contribution is picked up strongly depends on the polarization conditions of the experiment. This is of course very different from magnetic RIXS intensities at

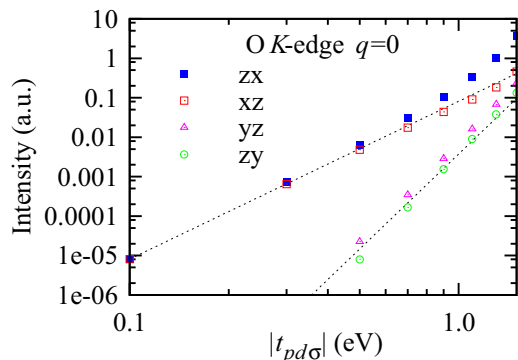


FIG. 4. (Color online) Magnetic RIXS intensity at the O  $K$  edge as a function of the Ir-O hopping  $t_{pd\sigma}$  on a log-log scale, for fixed  $\phi = 158^\circ$ . The two dotted lines represent proportionalities to  $t_{pd\sigma}^4$  and  $t_{pd\sigma}^8$ .

transition metal  $L$  edges and their polarization dependences, which are, in leading order, finite and independent of  $t_{pd\sigma}$ .

*Summary and conclusions.* We have shown on the basis of a symmetry analysis and exact diagonalization study that magnon scattering at O  $K$  edges becomes allowed when the inversion symmetry at the O site is broken, for instance, by a buckling of bonds. For cuprates the resulting magnetic RIXS intensity is tiny, but iridates may have the spin-orbit energy scale that is needed and also can fulfill the symmetry requirements. The first type of material that may come to

mind to observe single-magnon modes with oxygen  $K$ -edge RIXS are the quasi-2D iridates as  $\text{Sr}_2\text{IrO}_4$  and  $\text{Ba}_2\text{IrO}_4$ , in which  $L$ -edge RIXS has already established the presence of distinct magnon modes [10]. One can easily extend our symmetric analysis to the corresponding 2D lattices, which are still invariant under  $I_{\text{TM}}$  and break  $I_{\text{O}}$  when the  $\text{IrO}_4$  octahedra buckle. But even if the spin-orbit coupling and the Ir-O hybridization  $t_{pd\sigma}$  are significant in these materials, the Ir-O-Ir buckling angle for these systems is rather small, or even vanishing [32]. A better candidate system is the postperovskite  $\text{CaIrO}_3$ , in which a strong antiferromagnetic interaction along the  $c$  axis ( $J_c$ ) is present, where at the same time the corner-sharing octahedra are significantly buckled. Along the  $a$  axis the octahedra are edge sharing, which leads to weak ferromagnetic interactions so that, magnetically,  $\text{CaIrO}_3$  is a quasi-one-dimensional system [33,34], with  $|J_c/J_a| \gg 1$ . Even though the presence of a tetragonal field will cause the electronic state to deviate from a purely relativistic one [35] and implies some suppression of the single-magnon intensity takes place, it would be an ideal candidate to observe single-magnon RIXS at the oxygen  $K$  edge.

*Acknowledgments.* We thank Thorsten Schmitt and Giniyat Khaliullin for fruitful discussions. This work was supported by the Deutsche Forschungsgemeinschaft (DFG) through SFB 1143. B.H.K. was supported by the Basic Science Research Program through the National Research Foundation of Korea (NRF), funded by the Ministry of Education, Science and Technology (2013R1A6A3A0302053).

- [1] L. J. P. Ament, G. Ghiringhelli, M. M. Sala, L. Braicovich, and J. van den Brink, *Phys. Rev. Lett.* **103**, 117003 (2009).
- [2] L. Braicovich, L. J. P. Ament, V. Bisogni, F. Forte, C. Aruta, G. Balestrino, N. B. Brookes, G. M. De Luca, P. G. Medaglia, F. Miletto Granozio, M. Radovic, M. Salluzzo, J. van den Brink, and G. Ghiringhelli, *Phys. Rev. Lett.* **102**, 167401 (2009).
- [3] L. Braicovich, J. van den Brink, V. Bisogni, M. Moretti Sala, L. J. P. Ament, N. B. Brookes, G. M. De Luca, M. Salluzzo, T. Schmitt, V. N. Strocov, and G. Ghiringhelli, *Phys. Rev. Lett.* **104**, 077002 (2010).
- [4] L. J. P. Ament, M. van Veenendaal, T. P. Devereaux, J. P. Hill, and J. van den Brink, *Rev. Mod. Phys.* **83**, 705 (2011).
- [5] M. Le Tacon, G. Ghiringhelli, J. Chaloupka, M. Moretti Sala, V. Hinkov, M. W. Haverkort, M. Minola, M. Bakr, K. J. Zhou, S. Blanco-Canosa, C. Monney, Y. T. Song, G. L. Sun, C. T. Lin, G. M. De Luca, M. Salluzzo, G. Khaliullin, T. Schmitt, L. Braicovich, and B. Keimer, *Nat. Phys.* **7**, 725 (2011).
- [6] M. Le Tacon, M. Minola, D. C. Peets, M. Moretti Sala, S. Blanco-Canosa, V. Hinkov, R. Liang, D. A. Bonn, W. N. Hardy, C. T. Lin, T. Schmitt, L. Braicovich, G. Ghiringhelli, and B. Keimer, *Phys. Rev. B* **88**, 020501(R) (2013).
- [7] M. P. M. Dean, A. J. A. James, R. S. Springell, X. Liu, C. Monney, K. J. Zhou, R. M. Konik, J. S. Wen, Z. J. Xu, G. D. Gu, V. N. Strocov, T. Schmitt, and J. P. Hill, *Phys. Rev. Lett.* **110**, 147001 (2013).
- [8] M. P. M. Dean, G. Dellea, R. S. Springell, F. Yakhou-Harris, N. B. Kummer, K. Brookes, X. Liu, Y.-J. Sun, J. Strle, T. Schmitt, L. Braicovich, G. Ghiringhelli, I. Bozovich, and J. P. Hill, *Nat. Mater.* **12**, 1019 (2013).
- [9] L. J. P. Ament, G. Khaliullin, and J. van den Brink, *Phys. Rev. B* **84**, 020403(R) (2011).
- [10] J. Kim, D. Casa, M. H. Upton, T. Gog, Y.-J. Kim, J. F. Mitchell, M. van Veenendaal, M. Daghofer, J. van den Brink, G. Khaliullin, and B. J. Kim, *Phys. Rev. Lett.* **108**, 177003 (2012).
- [11] J. Kim, A. H. Said, D. Casa, M. H. Upton, T. Gog, M. Daghofer, G. Jackeli, J. van den Brink, G. Khaliullin, and B. J. Kim, *Phys. Rev. Lett.* **109**, 157402 (2012).
- [12] H. Gretarsson, J. P. Clancy, Y. Singh, P. Gegenwart, J. P. Hill, J. Kim, M. H. Upton, A. H. Said, D. Casa, T. Gog, and Y.-J. Kim, *Phys. Rev. B* **87**, 220407(R) (2013).
- [13] M. W. Haverkort, *Phys. Rev. Lett.* **105**, 167404 (2010).
- [14] M. van Veenendaal, [arXiv:1106.0640](https://arxiv.org/abs/1106.0640).
- [15] J.-i. Igarashi and T. Nagao, *Phys. Rev. B* **88**, 014407 (2013).
- [16] J.-i. Igarashi and T. Nagao, *Phys. Rev. B* **89**, 064410 (2014).
- [17] J. van den Brink, *Europhys. Lett.* **80**, 47003 (2007).
- [18] T. Nagao and J.-i. Igarashi, *Phys. Rev. B* **75**, 214414 (2007).
- [19] F. Forte, L. J. P. Ament, and J. van den Brink, *Phys. Rev. B* **77**, 134428 (2008).
- [20] J. P. Hill, G. Blumberg, Y.-J. Kim, D. S. Ellis, S. Wakimoto, R. J. Birgeneau, S. Komiya, Y. Ando, B. Liang, R. L. Greene, D. Casa, and T. Gog, *Phys. Rev. Lett.* **100**, 097001 (2008).

- [21] D. S. Ellis, J. Kim, J. P. Hill, S. Wakimoto, R. J. Birgeneau, Y. Shvyd'ko, D. Casa, T. Gog, K. Ishii, K. Ikeuchi, A. Paramekanti, and Y.-J. Kim, *Phys. Rev. B* **81**, 085124 (2010).
- [22] V. Bisogni, L. Simonelli, L. J. P. Ament, F. Forte, M. Moretti Sala, M. Minola, S. Huotari, J. van den Brink, G. Ghiringhelli, N. B. Brookes, and L. Braicovich, *Phys. Rev. B* **85**, 214527 (2012).
- [23] V. Bisogni, M. Moretti Sala, A. Bendounan, N. B. Brookes, G. Ghiringhelli, and L. Braicovich, *Phys. Rev. B* **85**, 214528 (2012).
- [24] B. J. Kim, H. Jin, S. J. Moon, J.-Y. Kim, B.-G. Park, C. S. Leem, J. Yu, T. W. Noh, C. Kim, S.-J. Oh, J.-H. Park, V. Durairaj, G. Cao, and E. Rotenberg, *Phys. Rev. Lett.* **101**, 076402 (2008).
- [25] B. J. Kim, H. Ohsumi, T. Komesu, S. Sakai, T. Morita, H. Takagi, and T. Arima, *Science* **323**, 1329 (2009).
- [26] See Supplemental Material at <http://link.aps.org/supplemental/10.1103/PhysRevB.92.081105> for details of the Hamiltonians and parametrizations of clusters with formally either  $\text{Ir}^{4+}$  or  $\text{Cu}^{2+}$  ions, and the numerical method.
- [27] B. H. Kim, G. Khaliullin, and B. I. Min, *Phys. Rev. Lett.* **109**, 167205 (2012).
- [28] B. H. Kim, G. Khaliullin, and B. I. Min, *Phys. Rev. B* **89**, 081109 (2014).
- [29] M. Imada, A. Fujimori, and Y. Tokura, *Rev. Mod. Phys.* **70**, 1039 (1998).
- [30] As a symmetry analysis, our calculation yields no single-magnon peak in the O  $K$ -edge RIXS spectra at  $q = \pi$ . The magnetic peak, however, is observed in the TM  $L$  edge at  $q = 0$ . See the Supplemental Material for details.
- [31] G. Jackeli and G. Khaliullin, *Phys. Rev. Lett.* **102**, 017205 (2009).
- [32] M. Moretti Sala, M. Rossi, S. Boseggia, J. Akimitsu, N. B. Brookes, M. Isobe, M. Minola, H. Okabe, H. M. Rønnow, L. Simonelli, D. F. McMorrow, and G. Monaco, *Phys. Rev. B* **89**, 121101(R) (2014).
- [33] N. A. Bogdanov, V. M. Katukuri, H. Stoll, J. van den Brink, and L. Hozoi, *Phys. Rev. B* **85**, 235147 (2012).
- [34] K. Ohgushi, J.-I. Yamaura, H. Ohsumi, K. Sugimoto, S. Takeshita, A. Tokuda, H. Takai, M. Takata, and T.-H. Arima, *Phys. Rev. Lett.* **110**, 217212 (2013).
- [35] M. M. Sala, K. Ohgushi, A. Al-Zein, Y. Hirata, G. Monaco, and M. Krisch, *Phys. Rev. Lett.* **112**, 176402 (2014).